Constraining the effectiveness of inherent tracers of captured CO_2 for tracing CO_2 leakage: Demonstration in a controlled release site

YeoJin Ju[1,2], Domokos Györe[3], Stuart M.V. Gilfillan[4], Seong-Sun Lee[1], Ilryoung Cho[1], Seung-Wook Ha[1], Won-Tak Joun[1], Hyun-Ji Kang[5], Hyun-Kwon Do[6], Dugin Kaown[1], Finlay M. Stuart[3], Doshik Hahm[7], Keyhong Park[8], Seong-Taek Yun[5], Kang-Kun Lee[1,]*

[1]School of Earth and Environmental Sciences, Seoul National University, 1 Gwanak-ro, Gwanak-gu, Seoul, 08826, South Korea.
[2]Disposal Safety Evaluation Research Division, Korea Atomic Energy Research Institute, Daejeon, Republic of Korea.
[3]Isotope Geosciences Unit, Scottish Universities Environmental Research Centre (SUERC), East Kilbride, G75 0QF, Scotland, United Kingdom
[4]School of GeoSciences, University of Edinburgh, Grant Institute, James Hutton Road, Edinburgh EH9 3FE, UK.
[5]Department of Earth and Environmental Sciences, Korea University, Seoul 02841, South Korea.
[6]Morwick G360 Groundwater Research Institute, College of Engineeringand Physical Sciences, University of Guelph, Guelph, ON N1G 2W1, Canada
[7]Department of Oceanography, Pusan National University, Busan, South Korea.
[8]Korea Polar Research Institute (KOPRI), Incheon, South Korea.

*Correspondence: kklee@snu.ac.kr

Abstract

Geological storage of carbon dioxide (CO_2) is an integral component of cost-effective greenhouse gas emissions reduction scenarios. However, a robust monitoring regime is necessary for public and regulatory assurance that any leakage from a storage site can be detected. Here, we present the results from a controlled CO_2 release experiment undertaken at the K-COSEM test site (South Korea) with the aim of demonstrating the effectiveness of the inherent tracer fingerprints (noble gases, $\delta^{13}C$) in monitoring CO_2 leakage. Following injection of 396 kg $CO_{2(g)}$ into a shallow aquifer, gas release was monitored for 2 months in gas/water phases in and above the injection zone. The injection event resulted in negative concentration changes of the dissolved gases, attributed to the stripping action of the depleted CO_2. Measured fingerprints from inherent noble gases successfully identified solubility-trapping of the injected CO_2 within the shallow aquifer. The $\delta^{13}C$ within the shallow aquifer could not resolve the level of gas trapping, due to the interaction with heterogeneous carbonate sources in the shallow aquifer. The time-series monitoring of $\delta^{13}C_{DIC}$ and dissolved gases detected the stripping action of injected $CO_{2(g)}$, which can provide an early warning of CO_2 arrival. This study highlights that inherent noble gases can effectively trace the upwardly migrating and fate of CO_2 within a shallow aquifer.

Keywords: Carbon capture and storage, monitoring, CO_2 leakage, inherent tracers, noble gas, solubility-trapping

Abstract Art

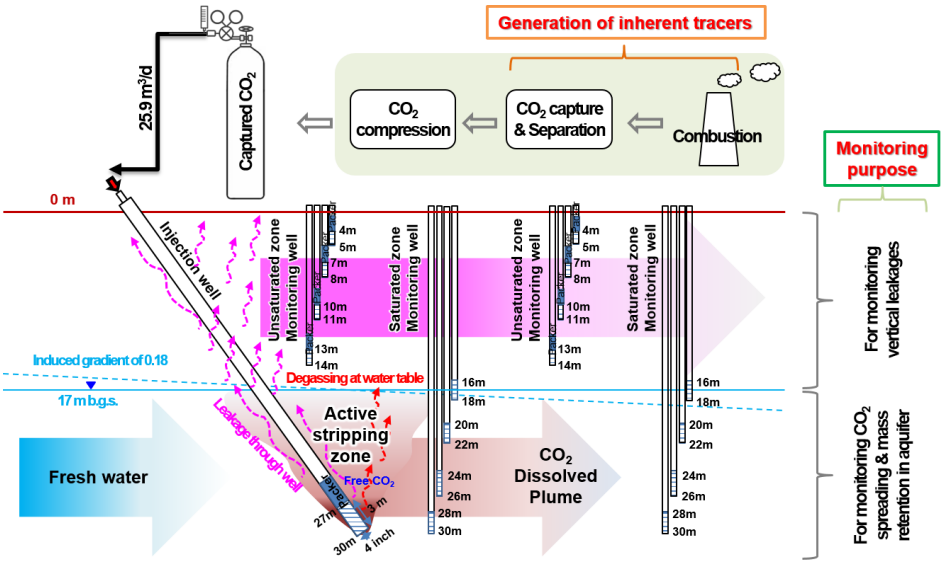

1. Introduction

To limit global warming to 1.5–2ºC relative to preindustrial levels (Azar et al., 2013; Haszeldine et al., 2005), mitigation technologies along with new emission related regulations, policies and standards have been developed (Bernstein et al., 2007; IPCC 2005). Carbon Capture and Storage (CCS) has the potential to substantially reduce anthropogenic CO_2 emissions over the coming decades (IEA, 2016; Wilberforce et al., 2019, 2021). However, the potential for upward migration of CO_2 from deep storage to surface is of public and regulatory concern (Bacon et al., 2016;; Kharaka et al., 2006, 2010; Little and Jackson, 2010; Zhang et al., 2017, 2019; Zheng et al., 2009). Public acceptance of geologic carbon sequestration will be gradually improved by demonstrating reliable monitoring techniques that provide assurance of long-term safety of reservoirs (Gholami et al., 2021; Van Alphen et al., 2007) and means of quantifying leakage in the event of unplanned gas escape (Holland and Gilfillan, 2013; Ju et al., 2019, 2020a, b).

Inert gases do not take part in chemical reactions and as they travel faster than CO_2 through pore space, they have been shown to be effective at providing an early-warning of the migration of CO_2 (Lu et al., 2012; Myers et al., 2013). Noble gases and halogenated compounds (e.g., SF_6, perfluorocarbons) have been widely tested as a means to 'fingerprint' injected CO_2, allowing it to be distinguished from CO_2 naturally present in the subsurface (Lu et al., 2012; Nimz and Hudson, 2005; Stalker et al., 2015; Trautz et al., 2013), and to verify whether the subsurface system is behaving as a conservative system for the volatiles (Ju et al., 2019, 2020a; Kim et al., 2018). However, halogenated compounds are potent greenhouse gases (Myers et al., 2013; Wells et al., 2007), and their usage is becoming increasingly restricted, which limits their large-scale use (Roberts et al., 2017). Noble gases are naturally present in subsurface fluids and their isotopic compositions are distinct between deep reservoirs and shallow

aquifers, meaning they are excellent candidates to trace the migration of deep-sourced CO_2 in the crust (Gilfillan and Haszeldine, 2011, Gilfillan et al., 2017, 2019; Györe et al., 2015, 2017, 2021; Karolytė et al., 2019; Mackintosh and Ballentine, 2012). The addition of dedicated noble gas tracers to the injected CO_2 has also been tested in different settings, highlighting their powerful ability to fingerprint injected CO_2 (Roberts et al., 2017; Stalker et al., 2015), and allowing mass balance constraints on leaked CO_2 to be obtained (; Holland and Gilfillan, 2013; Ju et al., 2019, 2020a, b).

The inherent noble gas composition of the injected CO_2 may also be used for monitoring purposes (Flude et al., 2016). This composition is the function of the source and the capture and purification process of the CO_2, but regardless, it is considerably different from most naturally sourced CO_2 (Flude et al., 2017). As the use of inherent tracers for CCS monitoring does not incorporate the process of adding artificial tracers into the injected CO_2, it offers a potentially cost effective monitoring of the injected CO_2. However, the effectiveness of the inherent tracing method must be comparable to that of artificial tracers (Ju et al., 2019, 2020a, 2020b), specifically: 1) whether it is robust enough to trace the spreading boundary of the CO_2 leak; 2) if it is useful for the provision of an early-warning of the spreading of leaking CO_2; 3) if it can successfully identify the fate of the CO_2 after leakage from the reservoir into shallower aquifers (solubility-trapping or loss into vadose/atmosphere).

In this study, a controlled CO_2 release experiment was performed at a shallow aquifer of Korea CO_2 Storage Environmental Management (K-COSEM) site. The design of the artificial injection test was intended to demonstrate the early-time vertical migration of sequestrated CO_2 before it achieved the equilibration with crustal fluids from deep geological reservoir. Following the artificial leakage, the CO_2 plume was subsequently formed in a shallow aquifer, which was used to investigate the feasibility of inherent tracers in detecting

leakage of injected CO_2. We measured the evolution of inherent tracers over time in response to CO_2 injection and the appearance of the CO_2 from multiple boreholes within vadose and aquifer zones. This allowed the effectiveness of inherent tracers as both early warning indicators of migrated CO_2, and whether these tools can provide mass balance estimates of the fate of the released CO_2 to be assessed.

2. Materials and Methods

2.1 Site description

The K-COSEM Research Center has developed a facility for controlled CO_2 release experiments at Eumseong-gun, South Korea (Figure 1a). Core sampling was performed during well-installation (Figure 1b) (Glew, 2002). Borehole (BHs) determined lithology down to the experimental depth (100 m) consists of medium to coarse silty sand (0–30 m below ground surface, bgs) and weathered biotite granite (30–70 m bgs), underlain by a consolidated bedrock (Lee et al., 2017b). The experimental layer at the depth of 30 m is dominated by quartz, albite, anorthite and microcline, with a small amount of carbonate units (Supplementary Material, Section S-1). A natural hydraulic gradient of 0.018 has been measured between the northeast and southwest ends of the experimental site (i.e., from BS-04 to BS-10) (Figure 1c). The aquifer was unconfined where the water table is located around 17 m bgs. Vertical and horizontal intrinsic permeability have been estimated to be between 1.76×10^{-12} and 1.24×10^{-14} cm/s around the injection depth as determined by an electrical resistivity survey (Lee et al., 2017a). This suggested a heterogeneous and anisotropic hydrological condition at this site. The hydrological setting of the site was investigated to understand its relation to the migration of volatile tracers. For example, a series of push and-pull tests was conducted in the unconfined aquifer using non-volatile tracer (Cl^-) and volatile tracer (SF_6), identifying that this unconfined

aquifer is not conservative for volatiles, indicated by a low recovery rate of SF_6 (Kim et al., 2018).

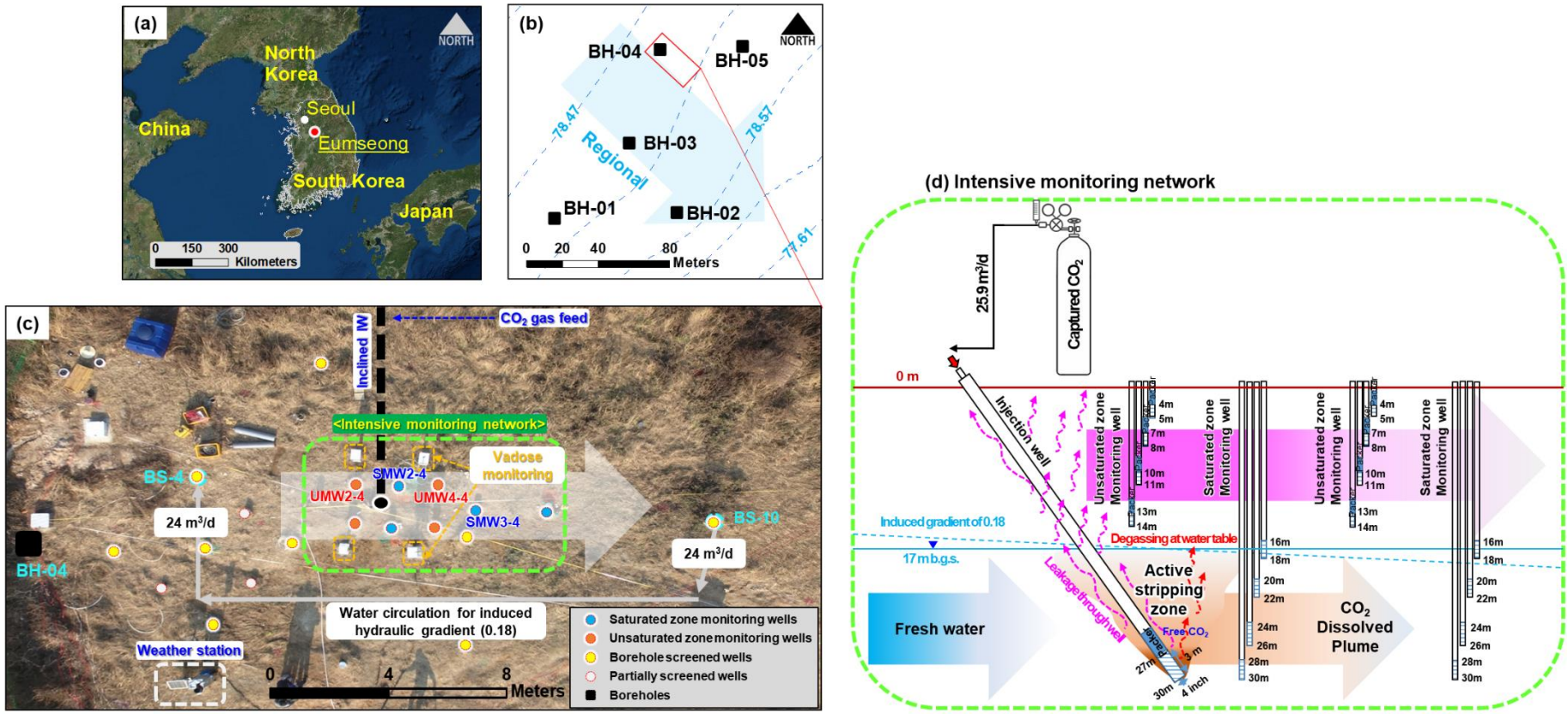

Figure 1. Maps of the K-COSEM CO_2 injection experiment site, South Korea. (a) The location of the study area. (b) Location map of BHs where core sampling was performed. (c) Design of controlled CO_2 release test where the groundwater was circulated using BS-4 and BS-10 to enhance the regional groundwater flow (Figure S1). (d) Configuration of three different monitoring media in test site such as: (1) saturated zone monitoring wells (SMWs) for dissolved phase CO_2, (2) borehole CO_2 gas monitoring and (3) unsaturated zone monitoring wells (UMWs) for monitoring the escaping budget of CO_2 from groundwater into atmosphere. Maps have been redrawn after Ju et al. (2019).

A previous artificial CO_2 and tracer injection test identified that a heterogeneous flow field exists in the shallow aquifer, which would complicate the migration pathway of the CO_2 plume (Ju et al., 2019). To overcome this issue, another test was performed in an induced flow gradient, 10 times above the level of the natural gradient, i.e., 0.18 (Figure S1). This allowed the migration pathway of the injected CO_2 to be focused into the intensive monitoring system resulting in increased monitoring efficiency (Figure 1c) (Ju et al., 2020a). In both injection tests, the behavior of the inert tracers was consistent with that of pCO_2, which implied that the distribution of migrated CO_2 was dominated by physical processes such as degassing, mixing and diffusive migration in the shallow aquifer (mineral adsorption/desorption were assumed to be negligible in the site based on the results of previous tests) (Ju et al., 2019, 2020a).

2.2. Design of controlled release test

A controlled release test was designed in order to test the effectiveness of inherent tracers within the injected CO_2. A total of 396 kg of gas phase CO_2, captured from a bioethanol production process line (in a liquor company), was injected into the shallow aquifer (at 27 m bgs) for 7 days, from 8–15th August 2019. Prior to the injection, the induced pressure gradient was formed as outlined above (Ju et al., 2020a) (Figure 1c). CO_2 injection was completed through an inclined injection well (IW) located inside an intensive monitoring network system (black dotted line in Figure 1c), in order to minimize the ascending of CO_2 through the well (Figure S1). The injection rate was controlled to be 6 L/min under a stable pressure of 0.14 atm above atmosphere and average ambient temperature of ~27°C. The injected gas was collected on site and analyzed for carbon and noble gas isotopes (Györe et al., 2015, 2017) (Supplementary Material, section S-2). The injection was performed 10 m below the water table, resulting in CO_2 pressure at the injection point to be > 2 atm.

A proportion of the $CO_{2(g)}$ was expected to dissolve into the groundwater and be transported along the induced hydraulic gradient, while the remainder was expected to migrate and be lost into the vadose zone. The CO_2 monitoring array comprised of two saturated zone monitoring wells (SMWs) and two unsaturated zone monitoring wells UMWs located within the intensive monitoring network (Figure 1c and 1d). The CO_2 was monitored in three different media: the vadose gas, the borehole gas and the dissolved phase (Figure 1d) (Supplementary Material, section S-2). CO_2 can reach the water table via diffusive migration or under the influence of buoyancy force (Figure 1d). The vadose zone monitoring wells were operating continuously using a real-time CO_2 monitoring system installed in UMWs in order to capture the escaping budget of CO_2 from groundwater to the vadose zone (Figure 1d) (Joun et al., 2019, 2020).

Samples for pCO_2-vadose, pCO_2-borehole, pCO_2-aquifer, $\delta^{13}C_{DIC}$ and dissolved gases such as O_2, ^{4}He, ^{20}Ne, ^{40}Ar and ^{84}Kr were taken 15 times during the ~2 month long sampling campaign (Figure S2). The pCO_2 of three different zones and dissolved oxygen (DO) were measured *in situ* while the isotopes of dissolved CO_2 and noble gases were measured in laboratories (Supplementary Material, section S-2). The measurements were carried out from SMW 2-4 (1.4 meters away from IW) and SMW 3-4 (3.6 meters away from IW). The hydrostatic pressure change was monitored continuously in order to maintain the induced hydraulic gradient and to monitor any pressure change during the experiment (Supplementary Material, section S-3).

3. Results and Discussion

3.1. pCO_2 and inherent tracers

3.1.1. Characteristics of noble gas tracers in the captured CO_2

The volumetric concentration of the inherent tracers of the captured CO_2 was much lower than that of air (Figure 2) after the CO_2 capture and purification process. Determined noble gas concentrations in the injected CO_2 showed 2-4 orders of depletion relative to the composition of air. The relative ratio of each gas to Ar is enriched in comparison to that of air, except for ^{20}Ne (Figure 2). These are in line with previous findings (Flude et al 2016, 2017) and is explained by the low solubility of noble gases, meaning that the vast majority are not captured by the capture process. However, whilst poorly soluble as a species, noble gas solubility in organic solvents or amine solutions increases with mass, yielding to a relative enrichment of heavy noble gases in CO_2 gas during the capture process (Figure 2). The depleted CO_2 gas was injected underground, which was expected to strip out the ambient groundwater and, lower the concentration of dissolved gases around the IW.

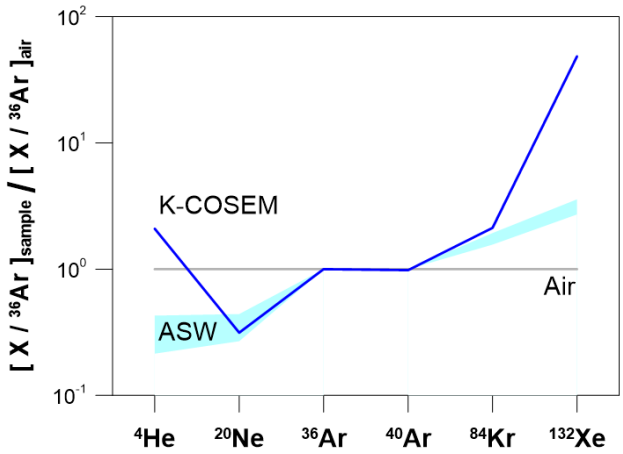

Figure 2. Composition of noble gas isotopes in captured and injected CO_2 gas used for the controlled release test. Three different compositions: 1) K-COSEM is the composition of the captured gas (blue curve); 2) ASW is the composition of air-saturated water analogous to a variety of natural groundwaters and 3) the atmospheric composition.

3.1.2. *p*CO_2 variations in three different monitoring media

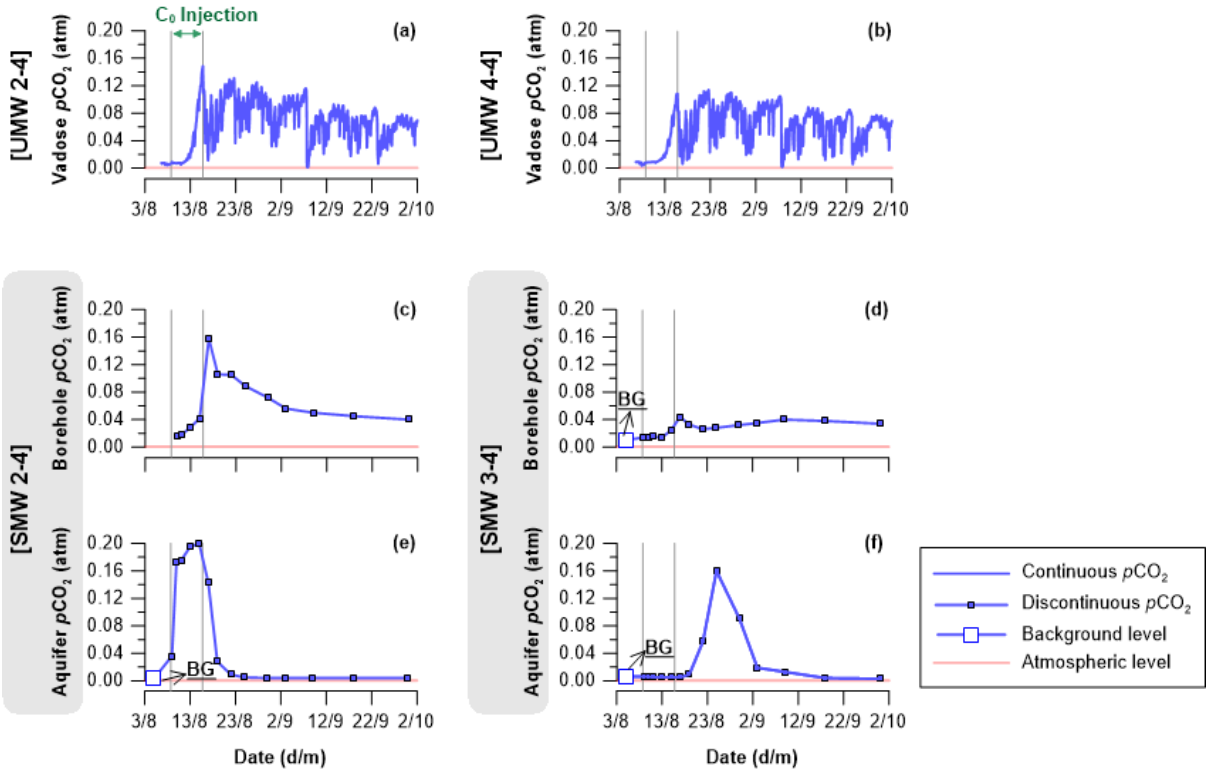

Figure 3. Time-series monitoring data of CO_2 partial pressure from three different media. Vertical grey lines indicate the CO_2 injection period and horizontal red line shows the atmospheric carbon dioxide level of 0.0004 atm. White squares present the background (BG) level of each component while small blue squares show the observations during the experiment. CO_2(g) was detected in the vadose well of UMW (a–b) and borehole gas inside the SMWs (c–d). Water samples were collected from SMWs and analyzed for dissolved CO_2 (e–f). The uncertainty of pCO_2 measurement was ±0.5% for borehole and ±3% for vadose zone monitoring and, better than 0.8% for aquifer CO_2.

In UMW 2-4, the maximum vadose zone CO_2 pressure was reached on the last day of injection at 0.15 atm (Figure 3a). UMW 4-4 exhibited an almost identical variation in CO_2 pressure as UMW 2-4, though the maximum CO_2 pressure of 0.11 atm was slightly lower than 0.14 atm at UMW 2-4. The vadose zone monitoring through a semi-open borehole illustrated a unique daily cycle of CO_2 concentration. This often showed a correlation with atmospheric pressure, demonstrating the action of barometric pumping on the CO_2 concentration within the vadose zone wells (Joun et al., 2019, 2020). This observation supported an earlier conclusion

that high frequency monitoring data is necessary for understanding the temporal variations of ground gas emissions and monitoring (Teasdale et al., 2014).

The CO_2 pressures within the borehole showed a gradual change during the injection period and reached up to 0.158 atm on 17th August 2019 (Figure 3c) at SMW 2-4. The CO_2 pressures at SMW 3-4 showed a relatively modest change up to 0.044 atm during the monitoring period (Figure 3d). It is interesting to note that the CO_2 pressure at SMW 3-4 showed a unique double peak, where the first peak (17th August 2019) was detected 23 days ahead of the second peak (9th September 2019) (Figure 3d).

The concentration of dissolved CO_2 immediately changed when CO_2 injection commenced (15th August 2019) (Figure 3e), which can be attributed to the location of SMW 2-4 within the CO_2 stripping zone (1.4 meters apart from the injection point; see Figure 1c). In SMW 3-4, the dissolved CO_2 showed a delayed response compared to that observed in SMW 2-4 (19th–22nd August 2019) (Figure 3f), attributed to its location further away from the injection point (3.6 meters apart; see Figure 1c). The maximum amount of dissolved CO_2 also varied between the locations (0.2 atm on 15th August 2019 for SMW 2-4; 0.16 atm on 25th August 2019 for SMW 3-4), where the CO_2 initially trapped near the injection point was diluted by mixing with local groundwater as it migrated.

In Figure 3, the vadose CO_2 showed smaller changes than the borehole/aquifer CO_2 in the stripping zone (i.e., SMW 2-4, Figure 3c and 3e), implying a vertical migration of CO_2 from aquifer to vadose zone. The arrival time of vadose CO_2 was almost identical to the borehole CO_2 in the stripping zone (Figure 3c), suggesting rapid vertical leakage. The initial increase in vadose CO_2 was 5 days behind the dissolved (aquifer) CO_2 (Figure 3e), implying that time is needed for the ascending CO_2 to spread and accumulate above the background CO_2 level in the vadose zone (red arrows in Figure 1d). The vadose CO_2 exhibited an identical

arrival time in the two UMWs (Figure 3a and 3b), which implies a rapid spreading of gas phase CO_2 through the vadose zone from above the injection point. These observations allow the behavior of the $CO_{2(g)}$ detected in UMWs to be conceptualized as follows: vadose CO_2 originated from 1) vertical leakage from the aquifer below (red arrows in Figure 1d) and/or 2) horizontal migration of CO_2 from vadose zone above the active leakage zone (pink arrows in Figure 1d).

In SMW 2-4, the borehole CO_2 had a delayed response of 2–7 days compared to the aquifer CO_2 (Figure 3c and 3e). Since SMW 2-4 is located near the injection point where active vertical leakage occurred (Figure 1c), this observation implied time was needed for CO_2 to vertically migrate and reach the water table within the monitoring well (blue arrows in Figure 1d). In SMW 3-4, the first peak was 5 days ahead of the arrival of the dissolved phase CO_2 (Figure 3d and 3f). At the time of initial injection period, a small amount of $CO_{2(g)}$ degassed from the groundwater and swiftly accumulated above the water table, while a minor amount of CO_2 dissolved in the groundwater. Following the initial injection period, the main peak (i.e., the second one) of borehole CO_2 (Figure 3d) was 15 days behind that of the dissolved CO_2 (Figure f), suggesting a slow diffusive emission of CO_2 gas from water table into the atmosphere, inside the monitoring well at this time (blue arrows in Figure 1d).

3.1.3. Early warning of inherent tracers for CO_2 arrival

The $\delta^{13}C_{DIC}$ decreased during the initial CO_2 injection period, which was attributed to the interaction between the local groundwater (-15.4 to -13.9‰) and the injected CO_2 of lighter $\delta^{13}C_{CO2}$ (-38.7‰) (Figure 4a and 4g). The results comply with previous studies (Raistrick et al., 2006; Schulz et al., 2012). Since the injected CO_2 was almost absent of other gases (Supplementary Material, section S-3), DO and noble gas tracers generally also decreased with

the injection event (Figure 4b–f and 4h–l), which shows the stripping action of injected CO_2. In SMW 2-4, the $\delta^{13}C_{DIC}$ and DO, ^{4}He, ^{20}Ne, ^{40}Ar and ^{84}Kr showed a consistent and rapid response linked with dissolved CO_2 during the injection period (Figure 4a–f). Over the monitoring period, the variations of the species showed much wider concaves in SMW 3-4 than in SMW 2-4 (Figure 4j–l). In SMW 3-4, the variation of the inherent gas tracers was different from that of the pCO_2 in the groundwater. The inherent gas tracers exhibited negative peaks over the course of sampling (Figure 4j–l) after CO_2 injection, while dissolved CO_2 showed a single spike (Figure 3f). For example, the inherent tracer fingerprints displayed the negative changes at 1–2 days after the injection commencement whilst the CO_2 arrivals were observed at 13–14 days after the injection. This can be attributed to the initial stripping of CO_2 gas causing the release of the dissolved gases into the vadose zone, which resulted in the early depletion for the inherent tracers ahead of CO_2 plume arrival in the groundwater monitoring well. This was also evidenced from the borehole CO_2, which showed an initial accumulation of pCO_2 in pressure-time curves prior to the CO_2 plume arrival (Figure 3d and 3f). The sensitive response of these inherent tracers indicates that such monitoring can provide an early warning of CO_2 arrival in the aquifer via groundwater monitoring wells.

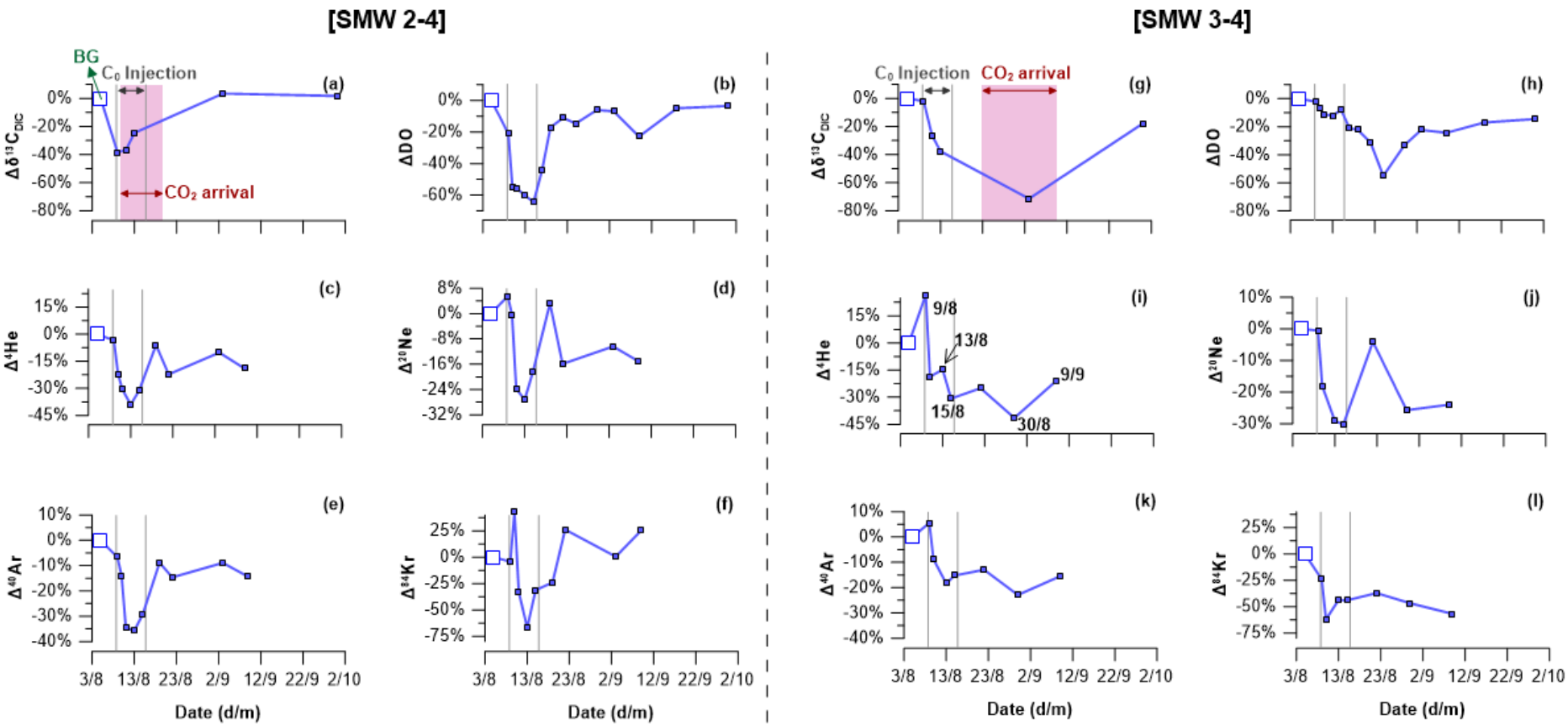

Figure 4. Time-series monitoring data of inherent tracers obtained from SMW series wells. Vertical grey lines indicate the CO_2 injection period. Red shadows display the pCO_2 peak periods monitored in the SMWs. White squares present the background level (BG) of each component while small blue squares show the observations during experiment. Relative change of concentration of each entity (C_i) was normalized to pre-injection concentration (C_0) such as (C_i- C_0)/ C_0 x 100. The inherent tracers were depleted following the injection event. Refer to Figure 1 for well locations. The precision of analytical measurement was better than 5% for noble gas tracers and the accuracy of $\delta^{13}C$ was ±0.3‰.

Interestingly, a small double peak is observed in ^{4}He within both wells within the sampling intervals, though SMW 3-4 also shows a marked change in ^{4}He concentration ahead of CO_2 plume arrival. ^{20}Ne values drop markedly in both wells on CO_2 injection, before rising and then falling again below their background levels. Notably both ^{40}Ar and ^{84}Kr values fall sharply on CO_2 injection in both wells, before returning to almost to the background levels in SMW 2-4, but not completely in SMW 3-4. The multiple bumps found in the time-series monitoring looked attributed to the heterogeneous permeability of the fields that provides diverse paths for CO_2 plume migrating in groundwater (Kilgallon et al., 2018; Lu et al., 2012). Furthermore, the diffusion process controls the migration of the inert species in groundwater, providing the most likely explanation for the different patterns of the different noble gas species (Ju et al., 2020a, 2020b). Therefore, the temporal variations of individual inherent tracers are affected by the number of paths they took in groundwater and, which are further differentiated by diffusion process.

3.2. Evolutionary path of CO_2 plume

Physical processes such as degassing, mixing and diffusive migration control the distribution of the CO_2 plume during its migration through the aquifer (Ju et al., 2020b). Noble gases have significantly different masses and hence are subject to mass dependent physical processes (Ballentine et al., 2002). The SMW 2-4 samples showed a sharp evolution in the pCO_2/Ar/He space (red line on Figure 5) after CO_2 injection. From 5th to 13th August, the pCO_2 rapidly increased with the CO_2 plume arrival while the He/Ar showed a relatively small change from 2.4 to 2.8 (Figure 5), which recovered back to the background level on 9th September 2019.

In SMW 3-4, further downstream from the injection well, the He/Ar ratio changed from 2.6 to 1.8 during the initial period of injection (blue line in Figure 5). The early

measurements of SMW 3-4 (i.e., 1.8–2.6 at 9th to 15th August) were located between the change observed in SMW 2-4 (i.e., 2.7 at 9th August) and the stabilized monitoring period of SMW 3-4 (i.e., 1.8 at 15th August), suggesting the mixing of the two water volumes in SMW 3-4 in the monitoring period. In the initial period, stripping action of CO_2 distinctly changed the composition of the noble gases near the injection point, generating a concentration gradient between the IW and the down-gradient monitoring wells. Then, along the concentration gradient between the locations, diffusive migration of the noble gases occurred. The speed of diffusive migration of each noble gas corresponds to their mass and diffusivity over a given concentration gradient, and therefore, resulted in the initial variation of He/Ar ratio at the CO_2 plume front. This observation corroborates the conclusion from a previous controlled release test using artificially enhanced tracers where the early-time variation (i.e., early arrival) of noble gas tracers could be partly attributed to the diffusive migration of these tracers (Ju et al., 2020a). In the stabilized period of SMW 3-4, the He/Ar ratio recorded the lowest value between 1.7 and 2.0 with the increased pCO_2 (Figure 5). Then, the composition of the CO_2 plume gradually recovered back to the initial baseline level of low pCO_2 (9th September 2019).

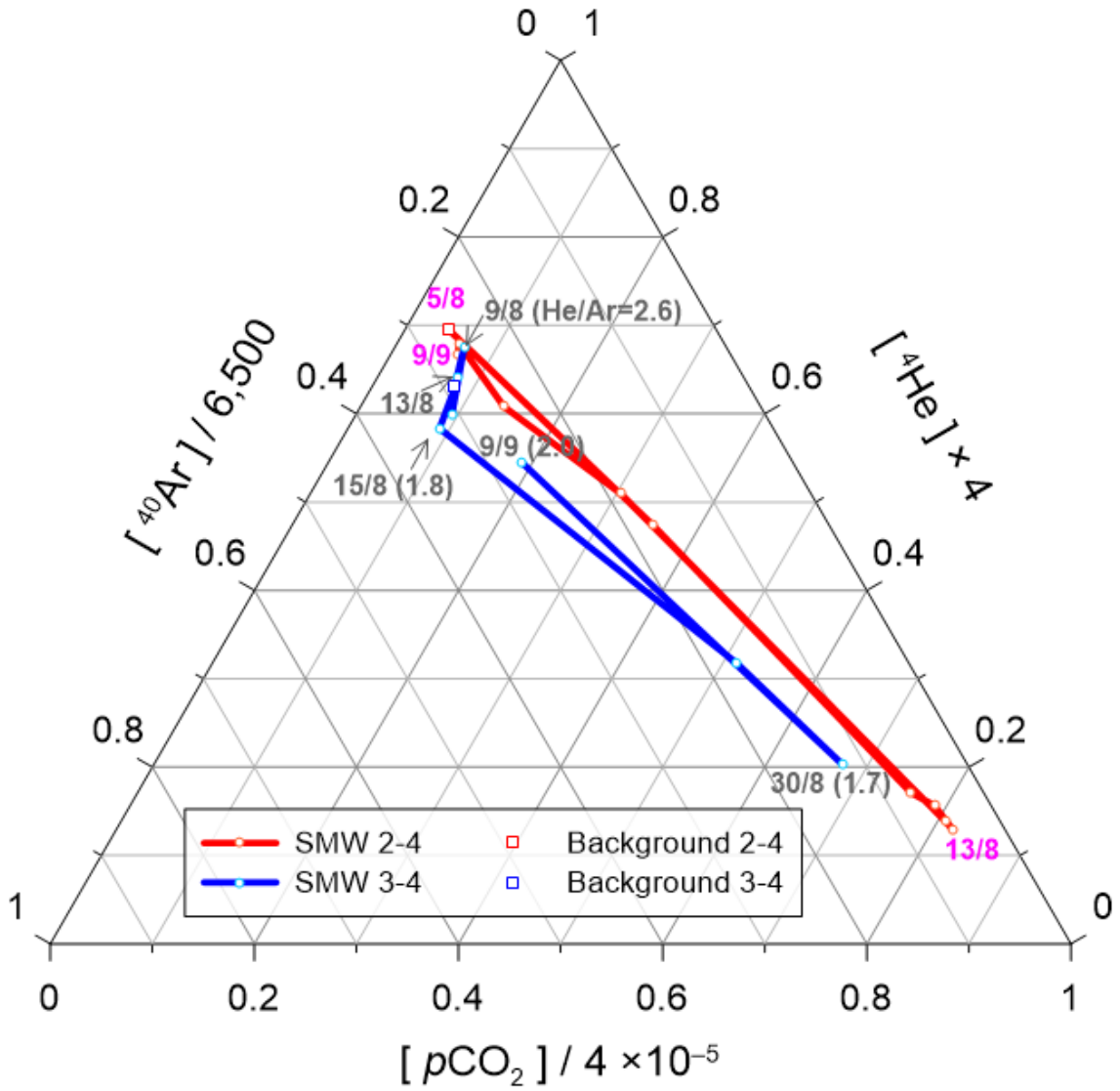

Figure 5. Evolution of the CO_2 plume depicted with ^{4}He, ^{40}Ar and pCO_2. While SMW 2-4 showed a sharp and linear increase in pCO_2 with CO_2 plume arrival, the SMW 3-4 showed the initial turbulence before the plume arrival. Dates shown as day/month.

3.3. CO_2 retention in shallow aquifers

Free-phase CO_2 released into a shallow groundwater aquifer is initially retained in the reservoir or released into the vadose zone, controlled by the solubility-trapping process (Ju et al., 2020b). The initial retention mechanisms are defined by physical processes, which can be identified using inert gas tracers (Ju et al., 2020a). In this experiment, He and Ar can be used to constrain the physical retention of the leaked CO_2. The two grey continuous lines depicted on Figure 6 show the predicted evolution of the He and Ar concentrations during degassing of

each species from the groundwater as the free phase CO_2 strips the groundwater aquifer at the site. This degassing of a groundwater body can occur via two means: 1) loss of free-phase CO_2 from groundwater in an open system; and 2) entrapment of the CO_2 gas, and resultant equilibrium in a closed groundwater system. In the study site, escaping CO_2 gas was clearly detected in the vadose zone monitoring system (Figure 3a and 3b), and hence the groundwater was not a closed system with respect to the injected CO_2. After the solubility-controlled process, the CO_2 plume was formed in the groundwater, which was markedly reduced in the other dissolved gases. The dotted lines on Figure 6 extending from the solubility-controlled evolution line-(1) (open system) highlight the fractionation trend that would be expected by dilution of the dissolved CO_2 by mixing with local groundwater after degassing of the groundwater had occurred (Supplementary Material, Section S-4).

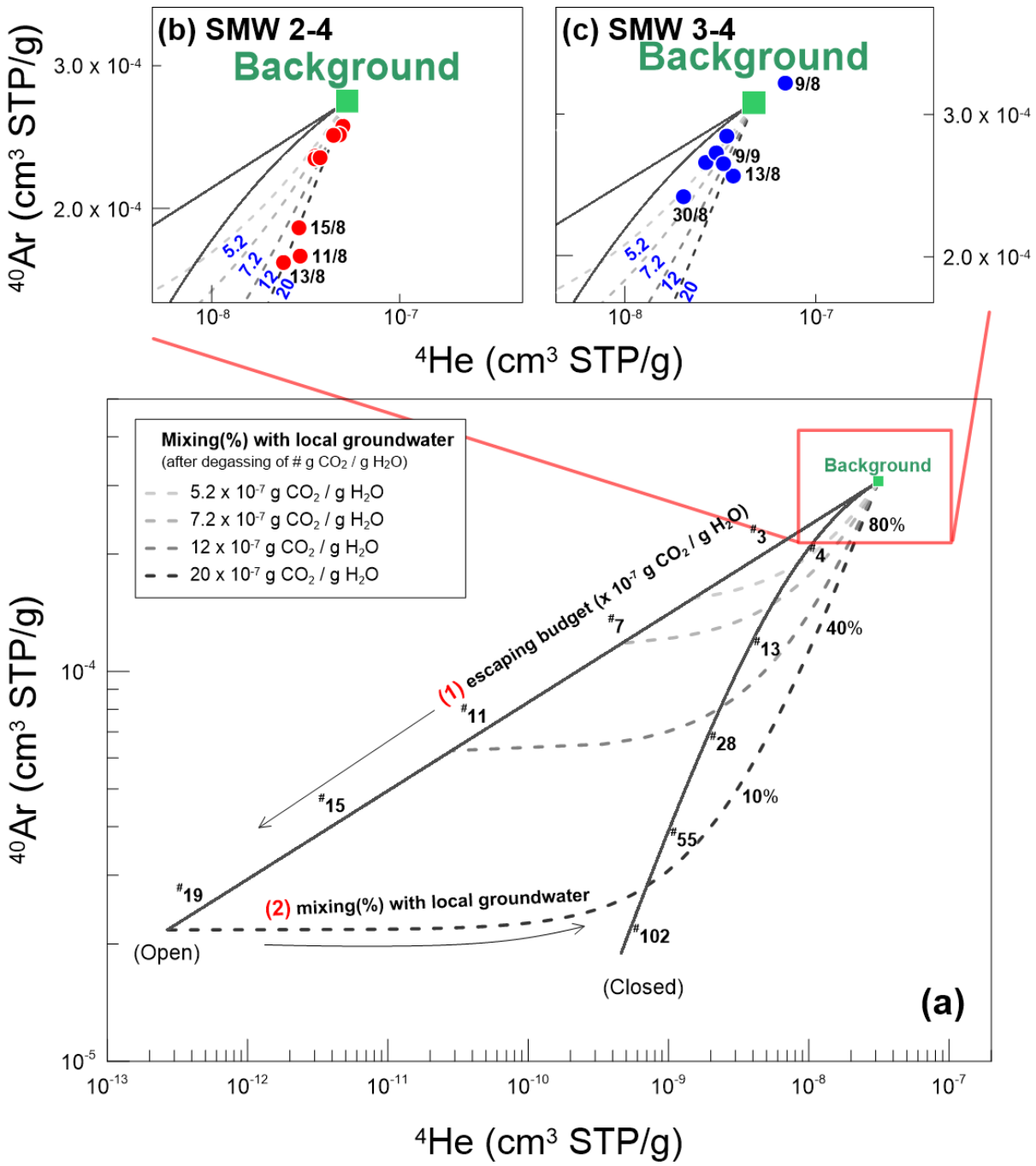

Figure 6. Modelled degassing loss of (^{4}He and ^{40}Ar) from the groundwater by injected free phase CO_2. The plume decreases the noble gas budget along the solid black line-(1), followed by mixing with local groundwater-(2). This degassing loss can be modelled via the two different scenarios of open and closed system gas loss from the groundwater. SMW 2-4 (b) and SMW 3-4 (c) experienced open system loss, as escaping CO_2 gas was clearly detected in the vadose zone. Dates shown as d/m. Measurement uncertainties are smaller than symbols. The repeatability of measurements was better than 5% for noble gas tracers.

The dissolved noble gases from SMW 2-4 and SMW 3-4 plot close to the background level (i.e., the green square on Figure 6b and 6c), suggesting that the sampled water was mostly

composed of local groundwater that was only partially impacted by the injected CO_2 (6–38% for SMW 2-4 and 17–44% for SMW 3-4). This can be attributed to the small size of the CO_2 plume formed in the groundwater (Figure S5). The samples from SMW 3-4 had a more dilute composition in comparison with the SMW 2-4 due to its location further away from the injection point (Figure 6b and 6c).

As all samples from both monitoring wells plot along the expected fractionation line, this shows that a two-step fractionation process occurred (Figure 6a): 1) the plume first underwent the stripping loss of He and Ar caused by free phase CO_2 and then; 2) dilution of the CO_2 plume by mixing with local groundwater. This corresponds to observations made from previous tests in the study site, using the addition of artificial noble gas tracers (Ju et al., 2019, 2020a).

The SMW 2-4 samples exhibit a relatively narrow range of CO_2 degassing loss into vadose zone, of 2.0×10^{-6} g CO_2/ g H_2O (Figure 6b). The SMW 3-4 samples showed a wider range of CO_2 loss than that of SMW 2-4, ranging from 5.2×10^{-7} to 2.0×10^{-6} g CO_2/ g H_2O (Figure 6c). The majority of SMW 3-4 samples locate in the volumetric mixing line indicating CO_2 loss of 5.2×10^{-7} g CO_2/ g H_2O into vadose zone that is lower than or overlap with the range of SMW 2-4. This can be attributed to the monitoring point of SMW 3-4 located further away from the CO_2 stripping zone caused by the injection well than that of SWM 2-4 (Figure 1c).

Unlike SWM 2-4, degassing due to CO_2 was not uniform around SMW 3-4. It was notable that the two observations made on the 13th August and 9th September 2019 did not lie on the theoretical line consistent with the other samples (Figure 6c). In SMW 3-4, the distribution of the CO_2 plume was not solely defined by the theoretical evolutionary path (i.e., from solubility-controlled process to volumetric mixing). This can be attributed to a diffusive migration of CO_2 plume, which has been often observed in boundaries of active degassing loss

zones in shallow aquifers (Ju et al., 2020a; Zhou et al., 2005). The diffusive mixing resulted in the signature of higher-degree CO_2 induced degassing (up to 2.0 x 10^{-6} g CO_2/ g H_2O) at the early stage (13th August 2019), suggesting that the plume front composition was impacted by diffusive migration from an active degassing zone. Combined with the results shown in the ternary diagram (the initial fluctuation of SMW 3-4 in Figure 5), this implies diffusive migration of the CO_2 plume from the SMW 2-4 (i.e., active loss zone) to SMW 3-4. The sample collected on 9th August 2019 appears to have captured more excess air than the previous background sample, however, this is still within the range expected for local background groundwaters (Ju et al., 2020c).

The total escaping budget of the free phase CO_2 from shallow aquifer groundwater can be estimated to be 0.29–0.41 kg based on the solubility-mixing evolution line (Supplementary Material, Section S-4). This amount is the portion of the injected CO_2 that contacted and interacted with the groundwater while escaping into the vadose zone.

Carbon isotopes can also be utilized to monitor the fate of CO_2 injected into groundwater reservoirs (Gilfillan et al., 2009; Humez et al., 2016). In this study, the $\delta^{13}C_{DIC}$ of produced groundwater gradually decreased from the background level (-15.4‰ to -13.9‰) in each monitoring well (Figure 4a and 4g) while interacting with injected $CO_{2(g)}$ with a low $\delta^{13}C_{CO2}$ (-38.7‰) value (Figure 7). In SMW 2-4, the largest change of $\delta^{13}C_{DIC}$ was expected to occur on the 13th of August 2019 based on the depletion of the inert gas tracers (Figure 4c–f). The estimated $\delta^{13}C_{DIC}$ was -24.5‰, which was lower than the observed value (i.e., -19.2‰) from SMW 2-4 (Supplementary Material, Section S-5). This deviation of $\delta^{13}C_{DIC}$, toward the carbonate dissolution line in Figure 7a, can be attributed to water-rock interaction, induced by CO_2 injection and subsequent pH decrease (4.0 without buffer). The largest change of $\delta^{13}C_{DIC}$ (i.e., -23.9‰) occurred on the 30th of August 2019 in SMW 3-4, which was more consistent with the estimation from the inert gas tracers (-23.5‰). This implied that less water-rock

interaction occurred in SMW 3-4 than in SMW 2-4, where carbonate dissolution enriched $\delta^{13}C_{DIC}$ in solution, controlled in part by the isotopic composition of local carbonate minerals (Canal et al., 2013; Dogramaci and Herczeg, 2002; Ha et al., 2020; Kirsch et al., 2014; Rightmire and Hanshaw, 1973).

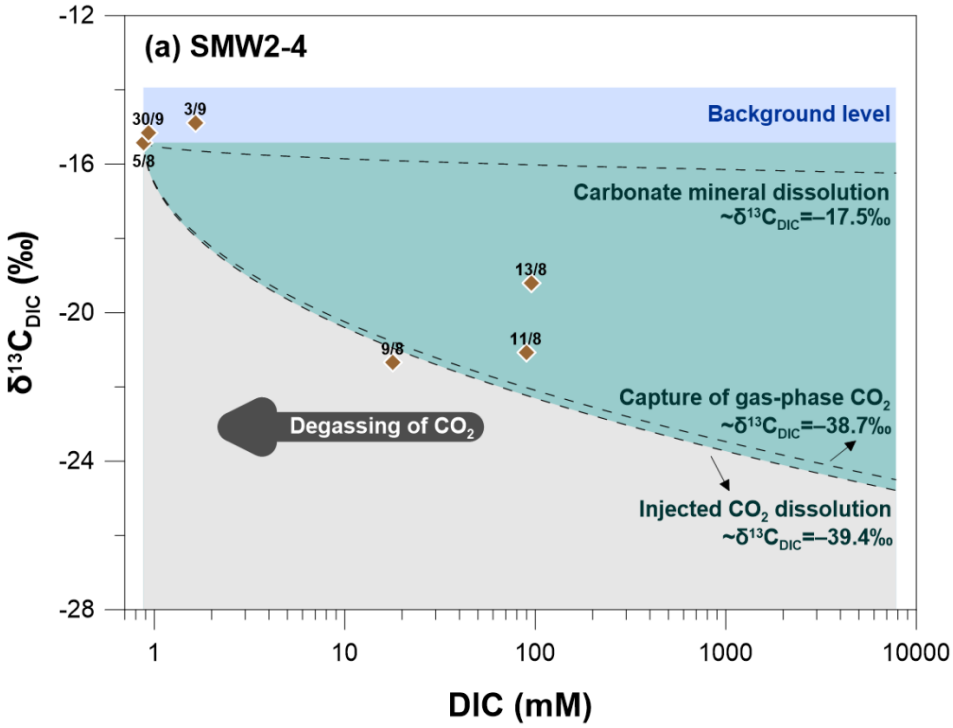

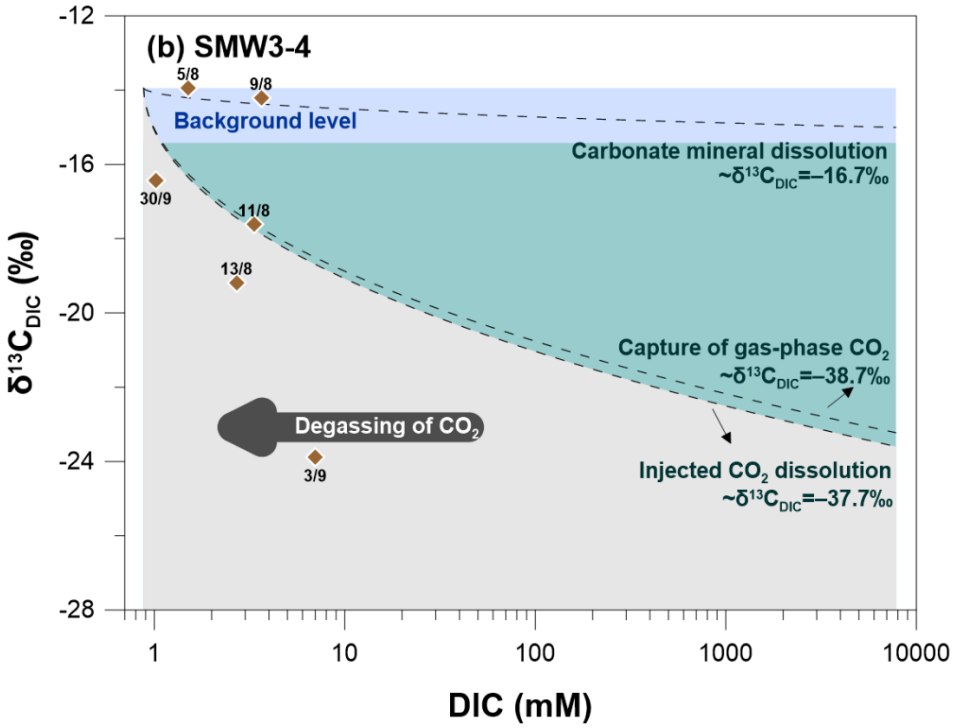

Figure 7 Evolution of $\delta^{13}C$ and DIC in a three-component mixing between (1) carbonate mineral dissolution, (2) injected CO_2 dissolution, and (3) capturing of injected CO_2. (a): SMW 2-4, (b): SMW 3-4. Note that there was no single process dominating the others, showing mixed compositions among the end-members. Samples below the dashed line-(3) (capturing of injected CO_2) went through a CO_2 degassing loss after dissolution. The accuracy of $\delta^{13}C$ measurement was ±0.3‰.

3.4. Implications for leakage monitoring

CCS pilot experiments have investigated the addition of artificial gas tracers into the CO_2 injection stream to increase the detection threshold for CO_2 leakage (Lu et al., 2012; Stalker et al., 2015). Recent studies and commercial CCS operations have used inherent tracers for the same purpose, which are economically more efficient than adding artificial tracers to the CO_2 (Flude et al., 2016).

From this controlled release study, we find that the inherent tracers exhibit a more prominent and rapid response to CO_2 migration than the monitored concentration of CO_2 in the vadose zone, borehole gas and groundwater (Figure 3 and 4). In particular, $\delta^{13}C_{DIC,}$ dissolved oxygen and dissolved noble gases demonstrated an early-stage depletion before CO_2 plume arrival in groundwater wells, exhibiting the initial loss of free phase CO_2 into the vadose zone. Whilst the stripping action of the injected CO_2 strongly depleted the inherent tracers, CO_2 did not accumulate in the groundwater (Figure 3 and 4). This observation was consistent with the previous artificial tracer-enhanced CO_2 injection tests (Ju et al., 2020a, 2020b), and suggests the potential effectiveness of inherent tracers to provide an early warning ahead of CO_2 arrival in groundwater aquifers. Additionally, we showed that the migration of inherent noble gases was dependent on diffusion at the plume front, along a concentration and hydraulic gradient between the active striping zone and local groundwater. According to the Fick's law, the slowly

spreading solute in groundwater relies on its molecular diffusion along the concentration gradient. This implied that the migrating speed of individual inherent tracers will be dependent on their concentration gradient formed from the stripping action of the depleted CO_2. If the gradient between CO_2 plume and ambient groundwater is steep enough, a low-density spatial monitoring around leak point will be enough to understand the trajectory of the depleted plume. Monitoring wells can be located according to site-specific risks, for example by selectively targeting areas of high permeability that potentially provide pathways for CO_2 transport. The mass-dependent movement arising from diffusion process, however, has also been observed even with small amount of CO_2 leakage (16.9 kg of CO_2) designed in natural flow conditions (Ju et al., 2019), implying the early warning of lighter noble gases for CO_2 arrival is promising.

While the CO_2 induced degassing loss in the groundwaters was verified from pCO_2-vadose, pCO_2-borehole and DO, quantitative evaluation of this was only possible through use of the noble gases. Monitoring of inert gas tracers allowed the evolutionary path of CO_2 plume in the solubility trapping-volumetric mixing curve to be determined (Figure 5). The size of CO_2 plume formed in the shallow aquifer was 143–205 m^3 of dissolved CO_2 and the dilution by local groundwater mixing was noticeable (> 56%) at only 3.4 m apart from the injection point. Despite the high dilution rate with the small scale of the leak, the inherent tracers produced measurable signals in groundwater monitoring wells more than 2 months, proving themselves useful in monitoring CO_2 leakage. Nevertheless, caution needs to be taken to delineate when observed change indicates leakage, as opposed to natural variation, which must be established prior to CO_2 injection through sufficiently long-term baseline monitoring.

The design of the artificial injection test was intended to demonstrate the early-time vertical migration of sequestrated CO_2 before it equilibrated with crustal fluids from deep geological reservoir. If CO_2 fluid achieved the equilibrium with the formation water at > 700 m depths, the noble gas signature gets rather enriched in crustal ^4He. In this case, the ^4He can

substitute the inherent tracers for monitoring the upward migration and the early warning the CO_2 arrival. This has been demonstrated in previous natural analogue studies using the noble gas tracers. For example, Gilfillan et al. (2011) used the crustal ^4He to demonstrate the upwelling of the deep crustal fluids into shallow natural reservoirs and, Gilfillan et al. (2017) applied the ^4He fingerprints to demonstrate the leak-tight reservoir near the Kerr-farm field.

In contrast to larger and deeper CO_2 tracing studies (Gilfillan et al., 2009; Györe et al., 2015, 2017; Mayer et al., 2013; Myrttinen et al., 2012; Zhang et al., 1995; Zhou et al., 2012), in our shallow aquifer experiment, solubility-controlled processes did not outweigh the water-rock interaction in controlling the $\delta^{13}C_{DIC}$ variation (Figure 7). This observation suggests $\delta^{13}C_{DIC}$ is not appropriate to evaluate the initial loss of $CO_{2(g)}$ into the vadose zone, which controls the overall size of CO_2 plume formed in shallow reservoirs. However, the early change of $\delta^{13}C_{DIC}$ prior to CO_2 plume arrival (Figure 3f and 4g) confirms the potential that this tracer provides a measure of the migration of the dissolved CO_2 front and could provide an early warning of CO_2 arrival in a groundwater aquifer. In contrast to $\delta^{13}C_{DIC}$, the noble gas ratios changed significantly with physical processes (i.e., degassing, volumetric mixing, diffusion), successfully demonstrating significant initial solubility-trapping of the injected CO_2 in the shallow aquifer.

After injecting 396 kg of $CO_{2(g)}$ into a shallow aquifer, the inherent tracer fingerprints remained detectable for more than 2 months in the groundwater, and which provided the long-term monitoring for understanding the CO_2 migration in subsurface system. Conclusively, the inherent tracer fingerprints showed a potential to replace the artificial tracer addition technique in terms of providing the early-warning of the CO_2 spreading and understanding the fate of the migrated CO_2 in shallow aquifer.

Acknowledgements

The study has been supported by a Korea Environmental Industry & Technology Institute (KEITI) grant entitled “R&D Project on Environmental Management of Geologic CO_2 Storage” (Project Number: 2018001810002), by a Korea Polar Research Institute grant (PE21110), by the National Research Foundation of Korea(NRF) grant funded by the Korea government(MSIT) (No. 2021R1C1C2006554) and, by Korea Environment Industry & Technology Institute(KEITI) through "Activation of remediation technologies by application of multiple tracing techniques for remediation of groundwater in fractured rocks" funded by Korea Ministry of Environment (MOE)(Grant number:20210024800002/148. We thank all the members of the K-COSEM team and, appreciate Intae Kim and Minjung Kim for their efforts and support on noble gas analysis.

REFERENCES

Azar, C., Johansson, D.J.A., Mattsson, N., 2013. Meeting global temperature targets-the role of bioenergy with carbon capture and storage. Environ. Res. Lett. 8 (3), 034004.

Bacon, D.H., Qafoku, N.P., Dai, Z.X., Keating, E.H., Brown, C.F., 2016. Modeling the impact of carbon dioxide leakage into an unconfined, oxidizing carbonate aquifer. Int. J. Greenh. Gas Con. 44, 290–299.

Ballentine, C.J., Burgess, R., Marty, B., 2002. Tracing fluid origin, transport and interaction in the crust. Rev. Mineral. Geochem. 47 (1), 539–614.

Bernstein, L., Roy, J., Delhotal, K.C., Harnisch, J., Matsuhashi, R., Price, L., Tanaka, K., Worrell, E., Yamba, F., Fengqi, Z., 2007. Industry, Lawrence Berkeley National Lab.(LBNL), Berkeley, CA (United States).

Canal, J., Delgado, J., Falcon, I., Yang, Q., Juncosa, R., Barrientos, V., 2013. Injection of CO_2-Saturated Water through a Siliceous Sandstone Plug from the Hontomin Test Site (Spain): Experiment and Modeling. Environ. Sci. Technol. 47 (1), 159–167.

Dogramaci, S.S., Herczeg, A.L., 2002. Strontium and carbon isotope constraints on carbonate-solution interactions and inter-aquifer mixing in groundwaters of the semi-arid Murray Basin, Australia. J. Hydrol. 262 (1–4), 50–67.

Flude, S., Gyore, D., Stuart, F.M., Zurakowska, M., Boyce, A.J., Haszeldine, R.S., Chalaturnyk, R., Gilfillan, S.M.V., 2017. The inherent tracer fingerprint of captured CO_2. Int. J. Greenh. Gas Con. 65, 40–54.

Flude, S., Johnson, G., Gilfillan, S.M.V., Haszeldine, R.S., 2016. Inherent Tracers for Carbon Capture and Storage in Sedimentary Formations: Composition and Applications. Environ. Sci.

Technol. 50 (15), 7939–7955.

Gholami, R., Raza, A., Iglauer, S., 2021. Leakage risk assessment of a CO_2 storage site: A review. Earth-Sci. Rev. 103849.

Gilfillan, S.M.V., Györe, D., Flude, S., Johnson, G., Bond, C.E., Hicks, N., Lister, R., Jones, D., Kremer, Y., Haszeldine, R., 2019. Noble gases confirm plume-related mantle degassing beneath Southern Africa. Nat. Commun. 10(1), 1–7.

Gilfillan, S.M.V., Haszeldine, R.S., 2011. Comment on "Potential Impacts of Leakage from Deep CO_2 Geosequestration on Overlying Freshwater Aquifers". Environ. Sci. Technol. 45 (7), 3171–3174.

Gilfillan, S.M.V., Sherk, G.W., Poreda, R.J., Haszeldine, R.S., 2017. Using noble gas fingerprints at the Kerr Farm to assess CO_2 leakage allegations linked to the Weyburn-Midale CO_2 monitoring and storage project. Int. J. Greenh. Gas Con. 63, 215–225.

Gilfillan, S.M.V., Sherwood Lollar, B., Holland, G., Blagburn, D., Stevens, S., Schoell, M., Cassidy, M., Ding, Z., Zhou, Z., Lacrampe-Couloume, G., Ballentine , C.J., 2009. Solubility trapping in formation water as dominant CO_2 sink in natural gas fields. Nature 458 (7238), 614–618.

Gilfillan, S.M.V., Wilkinson, M., Haszeldine, R.S., Shipton, Z.K., Nelson, S.T., Poreda, R., 2011. He and Ne as tracers of natural CO_2 migration up a fault from a deep reservoir. Int. J. Greenh. Gas Con. 5(6), 1507–1516.

Glew, J.R., Smol, J.P., Last, W.M., 2002. Sediment core collection and extrusion, in : Last, W.M., Smol, J.P. (Eds.), Tracking environmental change using lake sediments. Springer, Dordrecht, Netherlands, Vol. 1, pp 73–105.

Györe, D., Gilfillan, S.M.V., Stuart, F.M., 2017. Tracking the interaction between injected CO_2 and reservoir fluids using noble gas isotopes in an analogue of large-scale carbon capture and storage. Appl. Geochem. 78, 116–128.

Györe, D., Pujol, M., Gilfillan, S.M., Stuart, F.M., 2021. Noble gases constrain the origin, age and fate of CO_2 in the Vaca Muerta Shale in the Neuquén Basin (Argentina). Chem. Geol. 577, 120294.

Györe, D., Stuart, F.M., Gilfillan, S.M.V., Waldron, S., 2015. Tracing injected CO_2 in the Cranfield enhanced oil recovery field (MS, USA) using He, Ne and Ar isotopes. Int. J. Greenh. Gas Con. 42, 554–561.

Ha, J.H., Jeen, S.W., Hwang, H.T., Lee, K.K., 2020. Changes in geochemical and carbon isotopic compositions during reactions of CO_2-saturated groundwater with aquifer materials. Int. J. Greenh. Gas Con. 95 (95), 102961.

Haszeldine, R.S., Quinn, O., England, G., Wilkinson, M., Shipton, Z.K., Evans, J.P., Heath, J., Crossey, L., Ballentine, C.J., Graham, C., 2005. Natural geochemical analogues for carbon dioxide storage in deep geological porous reservoirs, a United Kingdom perspective. Oil Gas Sci. Technol. 60 (1), 33–49.

Holland, G., Gilfillan, S., 2013. Application of noble gases to the viability of CO_2 storage, in : Burnard, P. (Ed.), The noble gases as geochemical tracers. Springer, Berlin, Heidelberg, Germany, pp. 177–223.

Humez, P., Mayer, B., Ing, J., Nightingale, M., Becker, V., Kingston, A., Akbilgic, O., Taylor, S., 2016. Occurrence and origin of methane in groundwater in Alberta (Canada): Gas geochemical and isotopic approaches. Sci. Total Environ., 541, 1253–1268.

IEA, 2016. 20 Years of carbon capture and storage. Accelerating future deployment.

IPCC, 2005. Special report on carbon dioxide capture and storage. Cambridge University Press, UK and New York, USA, p. 14.

Joun, W.T., Lee, K.K., 2020. Reproducing natural variations in CO_2 concentration in vadose zone wells with observed atmospheric pressure and groundwater data. J. Environ. Manage. 266, 110568.

Joun, W.T., Rossabi, J., Shin, W.J., Lee, K.K., 2019. Real-time multi-level CO_2 concentration monitoring in vadose zone wells and the implication for detecting leakage events. J. Environ. Manage. 237, 534–544.

Ju, Y., Beaubien, S.E., Lee, S.S., Kaown, D., Hahm, D., Lee, S., Park, I.W., Park, K., Yun, S.T., Lee, K.K., 2019. Application of natural and artificial tracers to constrain CO_2 leakage and degassing in the K-COSEM site, South Korea. Int. J. Greenh. Gas Con. 86, 211–225.

Ju, Y., Gilfillan, S.M.V., Lee, S.-S., Kaown, D., Hahm, D., Lee, S., Park, I.-W., Ha, S.-W., Park, K., Do, H.-K., Yun, S.-T., Lee, K.-K., 2020a. Application of noble gas tracers to identify the retention mechanisms of CO_2 migrated from a deep reservoir into shallow groundwater. Int. J. Greenh. Gas Con. 97, 103041.

Ju, Y., Lee, S.-S., Kaown, D., Lee, K.-K., Gilfillan, S.M.V., Hahm, D., Park, K., 2020b. Noble gas as a proxy to understand the evolutionary path of migrated CO_2 in a shallow aquifer system. Appl. Geochem. 118, 104609.

Ju, Y., Massoudieh, A., Kaown, D., Yoon, Y.Y., Lee, K.K., 2020c. Characterization of flow dynamics around highly-utilized agricultural wells in a fractured-rock aquifer: Assessment of uncertainties lying on groundwater age-dating. J. Hydrol. 586, 124885.

Karolytė, R., Johnson, G., Györe, D., Serno, S., Flude, S., Stuart, F.M., Chivas, A.R., Boyce, A., Gilfillan, S.M.V., 2019. Tracing the migration of mantle CO_2 in gas fields and mineral water springs in south-east Australia using noble gas and stable isotopes. Geochim. Cosmochim. Acta 259, 109–128.

Kharaka, Y.K., Cole, D.R., Hovorka, S.D., Gunter, W.D., Knauss, K.G., Freifeld, B.M., 2006. Gas-water-rock interactions in Frio Formation following CO_2 injection: Implications for the storage of greenhouse gases in sedimentary basins. Geology 34 (7), 577–580.

Kharaka, Y., Campbell, P., Thorden, J., Thomas, P., Cole, D., Hovorka, S., 2010. Geologic storage of carbon dioxide: Potential environmental impacts of CO_2-organic interactions, Goldschmidt, Knoxville, Tennessee, USA (13–18 June), p. A511.

Kilgallon, R., Gilfillan, S.M.V., Edlmann, K., McDermott, C.I., Naylor, M., Haszeldine, R.S., 2018. Experimental determination of noble gases and SF_6, as tracers of CO_2 flow through porous sandstone. Chem. Geol. 480, 93–104.

Kim, H.-H., Lee, S.-S., Ha, S.-W., Lee, K.-K., 2018. Application of single-well push-drift-pull tests using dual tracers (SF_6 and salt) for designing CO_2 leakage monitoring network at the environmental impact test site in Korea. Geosci. J. 22 (6), 1041–1052.

Kirsch, K., Navarre-Sitchler, A.K., Wunsch, A., McCray, J.E., 2014. Metal Release from Sandstones under Experimentally and Numerically Simulated CO_2 Leakage Conditions. Environ. Sci. Technol. 48 (3), 1436–1442.

Lee, S.H., Kim, S.-O., Choi, B.-Y., Do, H.-K., Yun, S.-T., Jun, S.-C., 2017a. Hydrogeochemical modeling on water-rock-CO_2 interactions within a CO_2-injected shallow aquifer. J. Geol. Soc. Korea 53 (5), 657–673.

Lee, S.-S., Kim, H.-H., Joun, W.-T., Lee, K.-K., 2017b. Design and and construction of groundwater monitoring network at shallow-depth CO_2 injection and leak test site, Korea. Energy Procedia 114, 3060–3069.

Little, M.G., Jackson, R.B., 2010. Potential impacts of leakage from deep CO_2 geosequestration on overlying freshwater aquifers. Environ. Sci. Technol. 44 (23), 9225–9232.

Lu, J.M., Cook, P.J., Hosseini, S.A., Yang, C.B., Romanak, K.D., Zhang, T.W., Freifeld, B. M., Smyth, R.C., Zeng, H.L., Hovorka, S.D., 2012. Complex fluid flow revealed by monitoring CO_2 injection in a fluvial formation. J. Geophys. Res. Solid Earth 117 (B3).

Mackintosh, S.J., Ballentine, C.J., 2012. Using $^3He/^4He$ isotope ratios to identify the source of deep reservoir contributions to shallow fluids and soil gas. Chem. Geol. 304, 142–150.

Mayer, B., Shevalier, M., Nightingale, M., Kwon, J.-S., Johnson, G., Raistrick, M., Hutcheon, I., Perkins, E., 2013. Tracing the movement and the fate of injected CO_2 at the IEA GHG Weyburn-Midale CO_2 Monitoring and Storage project (Saskatchewan, Canada) using carbon isotope ratios. Int. J. Greenh. Gas Con. 16, S177–S184.

Myers, M., Stalker, L., Pejcic, B., Ross, A., 2013. Tracers - Past, present and future applications in CO_2 geosequestration. Appl. Geochem. 30, 125–135.

Myrttinen, A., Jeandel, E., Ukelis, O., Becker, V., van Geldern, R., Blum, P., Barth, J., 2012. Stable carbon isotope techniques to quantify CO_2 trapping under pre-equilibrium conditions and elevated pressures and temperatures. Chem. Geol. 320, 46–53.

Nimz, G., Hudson, G.B., 2005. The use of noble gas isotopes for monitoring leakage of geologically stored CO_2, in : Thomas, D.C., Benson, S.M. (Eds.), Carbon dioxide capture for storage in deep geologic formations. Elsevier, Thatcham, U.K., Vol. 2, pp. 1113–1130.

Raistrick, M., Mayer, B., Shevalier, M., Perez, R.J., Hutcheon, I., Perkins, E., Gunter, B., 2006. Using chemical and isotopic data to quantify ionic trapping of injected carbon dioxide in oil field brines. Environ. Sci. Technol. 40 (21), 6744–6749.

Rightmire, C.T., Hanshaw, B.B., 1973. Relationship between the carbon isotope composition of soil CO_2 and dissolved carbonate species in groundwater. Water Resour. Res. 9 (4), 958–967.

Roberts, J.J., Gilfillan, S.M.V., Stalker, L., Naylor, M., 2017. Geochemical tracers for monitoring offshore CO_2 stores. Int. J. Greenh. Gas Con. 65, 218–234.

Schulz, A., Vogt, C., Lamert, H., Peter, A., Heinrich, B., Dahmke, A., Richnow, H.H., 2012. Monitoring of a Simulated CO_2 Leakage in a Shallow Aquifer Using Stable Carbon Isotopes. Environ. Sci. Technol. 46 (20), 11243–11250.

Stalker, L., Boreham, C., Underschultz, J., Freifeld, B., Perkins, E., Schacht, U., Sharma, S., 2015. Application of tracers to measure, monitor and verify breakthrough of sequestered CO_2 at the CO2CRC Otway Project, Victoria, Australia. Chem. Geol. 399, 2–19.

Teasdale, C.J., Hall, J.A., Martin, J.P., Manning, D.A.C., 2014. Ground Gas Monitoring: Implications for Hydraulic Fracturing and CO_2 Storage. Environ. Sci. Technol. 48 (23), 13610–13616.

Trautz, R.C., Pugh, J.D., Varadharajan, C., Zheng, L., Bianchi, M., Nico, P.S., Spycher, N.F., Newell, D.L., Esposito, R.A., Wu, Y., Dafflon, B., Hubbard, S.S., Birkholzer, J.T., 2013. Effect of dissolved CO_2 on a shallow groundwater system: a controlled release field experiment. Environ. Sci. Technol. 47 (1), 298–305.

Van Alphen, K., tot Voorst, Q.v.V., Hekkert, M.P., Smits, R.E., 2007. Societal acceptance of

carbon capture and storage technologies. Energy Policy 35(8), 4368–4380.

Wells, A.W., Diehl, J.R., Bromhal, G., Strazisar, B.R., Wilson, T.H., White, C.M., 2007. The use of tracers to assess leakage from the sequestration of CO_2 in a depleted oil reservoir, New Mexico, USA. Appl. Geochem. 22 (5), 996–1016.

Wilberforce, T., Baroutaji, A., Soudan, B., Al-Alami, A.H., Olabi, A.G., 2019. Outlook of carbon capture technology and challenges. Sci. Total Environ., 657, 56–72.

Wilberforce, T., Olabi, A.G., Sayed, E.T., Elsaid, K., Abdelkareem, M.A., 2021. Progress in carbon capture technologies. Sci. Total Environ., 143203.

Zhang, J., Quay, P., Wilbur, D., 1995. Carbon isotope fractionation during gas-water exchange and dissolution of CO_2. Geochim. Cosmochim. Acta 59(1), 107–114.

Zhang, L.W., Parthasarathy, H., Karamalidis, A., 2017. Investigation on arsenopyrite dissolution and As (III) migration under geologic carbon storage conditions: A numerical simulation approach. Greenhouse Gases-Science and Technology 7 (3), 460–473.

Zhang, L., Wang, Y., Miao, X., Gan, M., Li, X., 2019. Geochemistry in geologic CO_2 utilization and storage: A brief review. Advances in Geo-Energy Research 3 (3), 304–313.

Zheng, L.G., Apps, J.A., Zhang, Y.Q., Xu, T.F., Birkholzer, J.T., 2009. On mobilization of lead and arsenic in groundwater in response to CO_2 leakage from deep geological storage. Chem. Geol. 268 (3-4), 281–297.

Zhou, Z., Ballentine, C.J., Kipfer, R., Schoell, M., Thibodeaux, S., 2005. Noble gas tracing of groundwater/coalbed methane interaction in the San Juan Basin, USA. Geochim. Cosmochim. Acta 69 (23), 5413–5428.